

NANO EXPRESS

Open Access



# Positive and Negative Photoconductivity Conversion Induced by H<sub>2</sub>O Molecule Adsorption in WO<sub>3</sub> Nanowire

Yahui Liu, Peng Fu, Yanling Yin, Yuehua Peng, Wenjun Yang, Gang Zhao, Weike Wang, Weichang Zhou and Dongsheng Tang\*

## Abstract

Negative photoconductivity effect has been observed in the Au/WO<sub>3</sub> nanowire/Au devices in a high humidity environment, which might be attributed to the accumulation of H<sup>+</sup> ions on the surface of WO<sub>3</sub> nanowire. Under illumination with violet light (445 nm), the photo-excited holes can oxidize the adsorbed H<sub>2</sub>O molecules to produce H<sup>+</sup> ions and O<sub>2</sub>, while the photo-excited electrons at the conduction band bottom do not have enough energy to reduce H<sup>+</sup> ions. These H<sup>+</sup> ions will accumulate on the surface of the hexagonal WO<sub>3</sub> nanowire. They will capture mobile electrons and then reduce the concentration of carriers, which will result in a significant increase in the height of interface barrier and then a significant decrease in the conductance of the Au/h-WO<sub>3</sub> nanowire/Au device. By adjusting the relative humidity, light intensity, or bias voltage, the concentration and distribution of H<sup>+</sup> ions and then the conversion between positive and negative photoconductivity, as well as resistive switching properties, can be well regulated in this kind of devices.

**Keywords:** Hexagonal WO<sub>3</sub> nanowire, Negative photoconductivity, Positive photoconductivity, Hydrogen ion, Schottky emission

## Introduction

Tungsten oxide (WO<sub>3</sub>) exhibits excellent photo-(electro-, gas-, thermo-)chromic properties and resistive switching behaviors [1–13], which might be attributed to its distinctive crystal and electronic band structures. WO<sub>3</sub> is constructed from WO<sub>6</sub> octahedra by sharing the equatorial oxygen atoms, which leaves more empty interstices in the oxygen sub-lattice. As a result, WO<sub>3</sub> can accommodate external species such as hydrogen ions and alkali metal ions into its solid framework to form stable nonstoichiometric intercalation compounds with the color from yellowish green to gold and the conductivity from insulator to metal. Meanwhile, the bottom of the conduction band of WO<sub>3</sub> lies below the hydrogen ion reduction level, while the top of the valence band lies above the level of H<sub>2</sub>O molecular oxidation. Therefore, H<sub>2</sub>O molecules

adsorbed on the surface of WO<sub>3</sub> can be oxidized to produce hydrogen ions (H<sup>+</sup> ions) and O<sub>2</sub> by the excited or injected holes at the top of the valence band, while H<sup>+</sup> ions cannot be reduced by electrons at the bottom of the conduction band. Generally speaking, the coloring or resistive switching of WO<sub>3</sub> in atmospheric environment under external excitation such as illumination and bias voltage can be attributed to the H<sup>+</sup> ions embedded in the lattice [14, 15].

Therefore, it is possible to manipulate the optical and resistive switching properties of WO<sub>3</sub> by regulating the transport and distribution of H<sup>+</sup> ions in the lattice or on the surface of WO<sub>3</sub>. Single crystalline hexagonal WO<sub>3</sub> nanowire (h-WO<sub>3</sub> NW) possessing large specific surface area and conductive channel might be an ideal platform for studying the effect of the H<sup>+</sup> ions produced by H<sub>2</sub>O oxidation. In our previous work, the single-crystalline h-WO<sub>3</sub> NWs grown along the *c* direction do exhibit memristive effect or resistive switching phenomenon, which can be enhanced remarkably and even regulated by

\* Correspondence: [dstang@hunnu.edu.cn](mailto:dstang@hunnu.edu.cn)

Synergetic Innovation Center for Quantum Effects and Application, Key Laboratory of Low-dimensional Quantum Structures and Quantum Control of Ministry of Education, School of Physics and Electronics, Hunan Normal University, Changsha 410081, People's Republic of China

the  $H^+$  ions produced by the oxidation of the adsorbed  $H_2O$  molecules [16–19].

In this letter, we explored the photoconductivity of h- $WO_3$  NW under different relative humidity and found that the positive photoconductivity (PPC) effect is always accompanied by negative photoconductivity (NPC) effect in a high relative humidity environment. By adjusting the relative humidity, light intensity, or bias voltage, it is possible to manipulate the creation, distribution, and annihilation of  $H^+$  ion on the surface of  $WO_3$  and then regulate the concentration of carriers in the  $WO_3$  nanowire and the height of the interface barrier.

## Methods

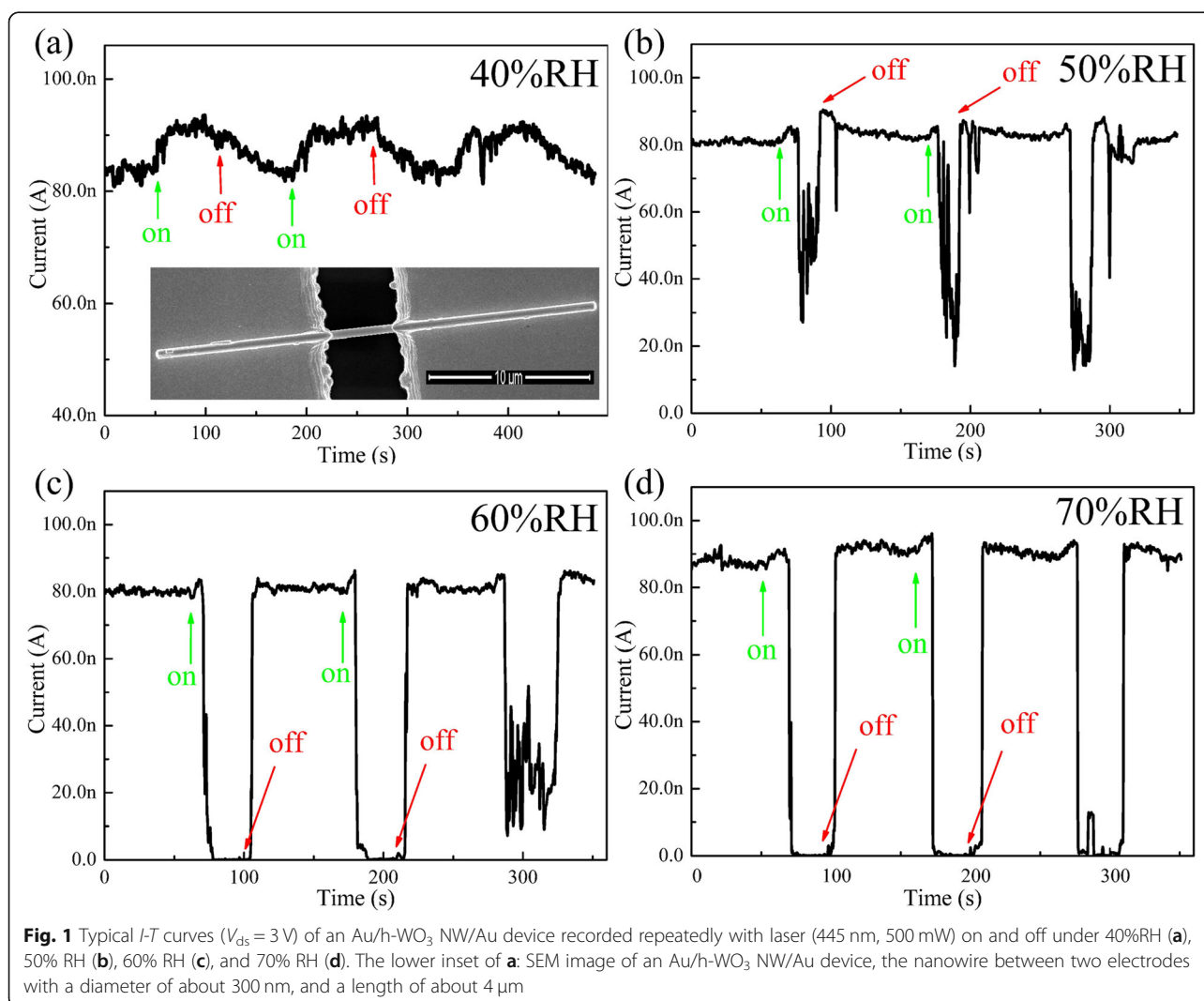
### $WO_3$ Nanowire Synthesis

The h- $WO_3$  nanowires used in this investigation were synthesized using a simple hydrothermal method as previously reported [20, 21]. In a typical synthesis, 8.25 g sodium tungstate ( $Na_2WO_4 \cdot 2H_2O$ ) was dissolved in 250

mL deionized water. Hydrochloric acid (HCl, 3 M) was used to adjust the PH value of the  $Na_2WO_4$  solution to 1.2. After being filtered, the precipitate was washed sequentially with deionized water and ethanol to remove contaminant ions and then dispersed in 200 mL citric acid ( $C_6H_8O_7$ , 0.1 M) to form a translucent homogeneous and stable  $WO_3$  sol. A 45-mL volume of  $WO_3$  sol was transferred into a 50-mL autoclave, and then 1.3 g potassium sulfate ( $K_2SO_4$ ) was added to the sol. The autoclave was sealed and maintained at 240 °C for 32 h, and then cooled down to room temperature. The precipitates in the solution were filtered, washed sequentially with deionized water and ethanol to remove possible remnant ions, and then dried at 60 °C.

### Device Fabrication

The individual h- $WO_3$  nanowire-based devices were fabricated on heavily n-doped Si substrate covered with a 100 nm thick thermally grown  $SiO_2$  layer. Electrodes were



defined on the Si substrate with WO<sub>3</sub> nanowires by using a standard photo-lithography technique (ABM, Inc., San Jose, CA (405)) and formed by metal deposition (100-nm-thick Au) and a lift-off process.

**Electrical Measurement**

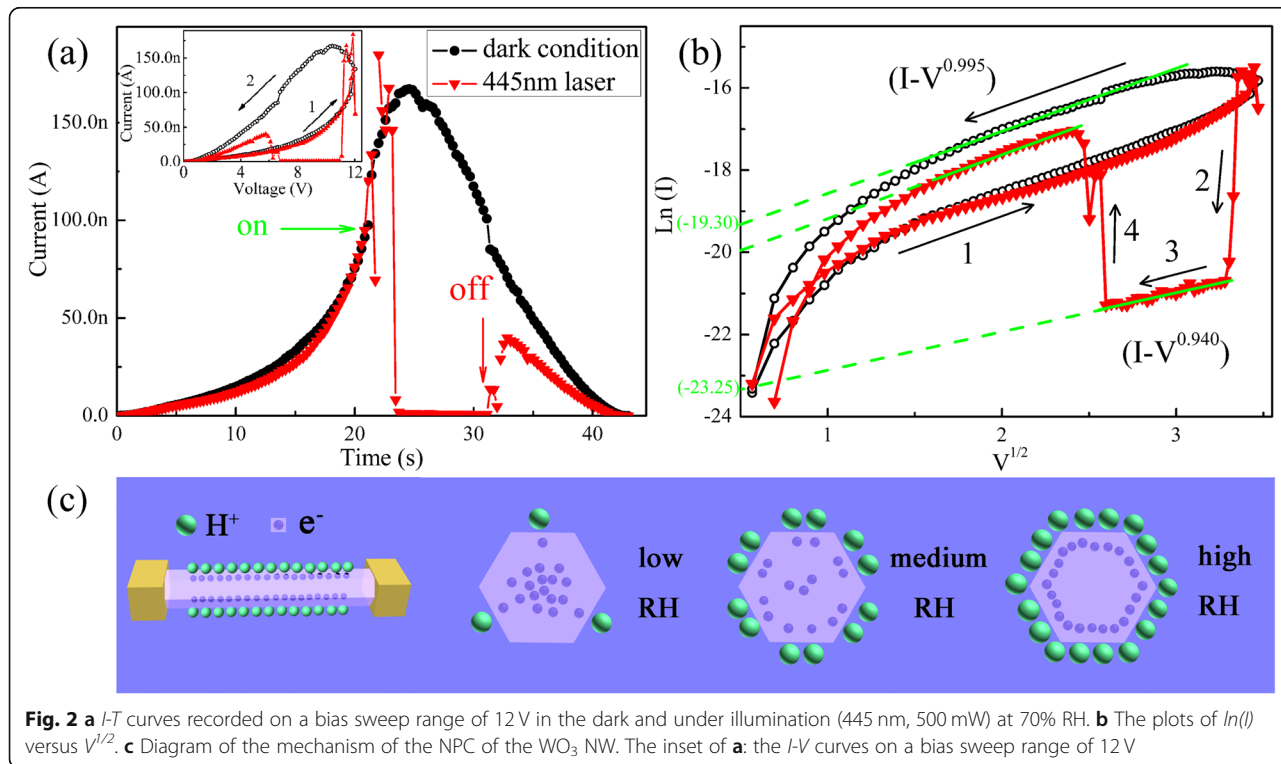
Electrical transport measurements were conducted on a probe station at room temperature by using semiconductor characterization systems (Keithley 2602). The probe station is placed in a homemade vacuum chamber, which is firstly vacuumized to a base pressure less than 10<sup>-1</sup> Pa by a mechanical pump. The relative humidity (RH) in the environment was adjusted by evaporation of deionized H<sub>2</sub>O and a dehumidifier. The accuracy of the humidity sensor used in our experiments was about ± 1%.

**Results and Discussion**

Figure 1 shows the typical current-time (*I*-*T*) curves of an Au/h-WO<sub>3</sub> NW/Au device recorded with laser (445 nm, 500 mW) on and off under different RH levels. When the RH is 40% (Fig. 1a), the current rises slightly under illumination, which is the normal PPC due to the inter-band transition [22, 23]. As the RH increases to 50% (Fig. 1b), the current rises slightly when the laser is turned on. And then, after about 10 s, the photocurrent drops significantly, namely the intriguing NPC effect. With increasing the RH gradually, the device exhibits the more excellent and stable NPC as shown in Fig. 1c, d. The NPC effect has been reported in some nanomaterials [24–26], but never

been observed in WO<sub>3</sub>. Preliminarily, the NPC effect of WO<sub>3</sub> nanowire might be attributed to the adsorbed H<sub>2</sub>O molecules on the surface. After all, H<sub>2</sub>O molecule adsorption and photo-desorption have been proved to play an important role in determining the photoelectric properties and lead to NPC effect in nanoscale materials [27–29]. It means that the conductance of these nanoscale materials depend sensitively on the amount of adsorbed H<sub>2</sub>O molecules. However, unlike the photocurrents, the dark currents recorded under the different RH levels are almost the same (80 nA) as shown in the Fig. 1, which proves that the changes in the photocurrents under different RH levels cannot simply be attributed to photo-induced desorption H<sub>2</sub>O molecules. Therefore, there is a new physical mechanism answering for the NPC effect of the h-WO<sub>3</sub> NW. In addition, the dark current in Fig. 1d is slightly larger than 80 nA. When the RH is very high, more H<sub>2</sub>O molecules are adsorbed on the WO<sub>3</sub> NW and can form the H<sub>2</sub>O film on the surface of WO<sub>3</sub>. And this layer of water molecule can increase the conductance of the device based on the Grotthuss mechanism [30]. Therefore, the dark current in Fig. 1d increases slightly.

To elucidate the origins of the NPC, the involving conductive mechanism needs to be determined firstly. As shown in the inset of Fig. 2a, the typical current-voltage (*I*-*V*) curve is recorded with the bias voltage scanning and the laser on and off under the 70% RH, which indicates NPC effect as well as resistive switching. For the purpose of making an obvious contrast, the *I*-*V* curves were



converted to the  $I$ - $T$  curves as displayed in Fig. 2a and replotted based on the Schottky law ( $\ln I \propto V^{1/2}$ ) [31]. For both photocurrent and dark current,  $\ln I$  is linear with  $V^{1/2}$  under high bias voltage. The conduction mechanisms for both cases are Schottky emission and barrier height which can be obtained from the intercept of the Schottky plot. The Schottky barrier under light illumination is much higher than that in dark environment as indicated by the green intercepts in Fig. 2b. Therefore, the NPC effect of the h-WO<sub>3</sub> NW might be attributed to the increase of the Schottky barrier height induced by violet light illumination. As previously reported [15], the resistive switching properties this kind of devices has can be enhanced remarkably by adsorbed H<sub>2</sub>O molecules. In that situation, the holes injected from the positively charged electrode oxidize the adsorbed H<sub>2</sub>O molecules producing H<sup>+</sup> ions and O<sub>2</sub>, while the electrons injected from the negatively charged electrode under small bias voltage do not have enough energy to reduce H<sup>+</sup> ions because of the peculiar electronic band structure of WO<sub>3</sub>. The H<sup>+</sup> ions produced

by H<sub>2</sub>O oxidation will accumulate gradually on the surface under continuous bias scanning, which will deplete all mobile electrons in the WO<sub>3</sub> nanowire. Therefore, under illumination with violet light (445 nm), the photo-excited holes can also oxidize the adsorbed H<sub>2</sub>O molecules to produce H<sup>+</sup> ions. The only difference is that the H<sup>+</sup> ions are produced and accumulated faster, which prevents H<sup>+</sup> ions from entering the lattice of WO<sub>3</sub> NW more easily to transform it into a metallic state. They will capture mobile electrons to form the electric double-layer and then reduce the concentration of carriers as shown in Fig. 2c, which will result in a significant increase in the height of interface barrier and then a significant decrease in the conductance of the Au/h-WO<sub>3</sub> NW/Au device. If the RH level is low (less than 50%), there are less than two H<sub>2</sub>O molecular layers on the surface, and the amount of H<sup>+</sup> ions produced by water oxidation is relatively small. Furthermore, H<sup>+</sup> ions cannot move freely in the discontinuous layers of H<sub>2</sub>O molecules to accumulate near the negatively charged electrode. Accordingly the ability of

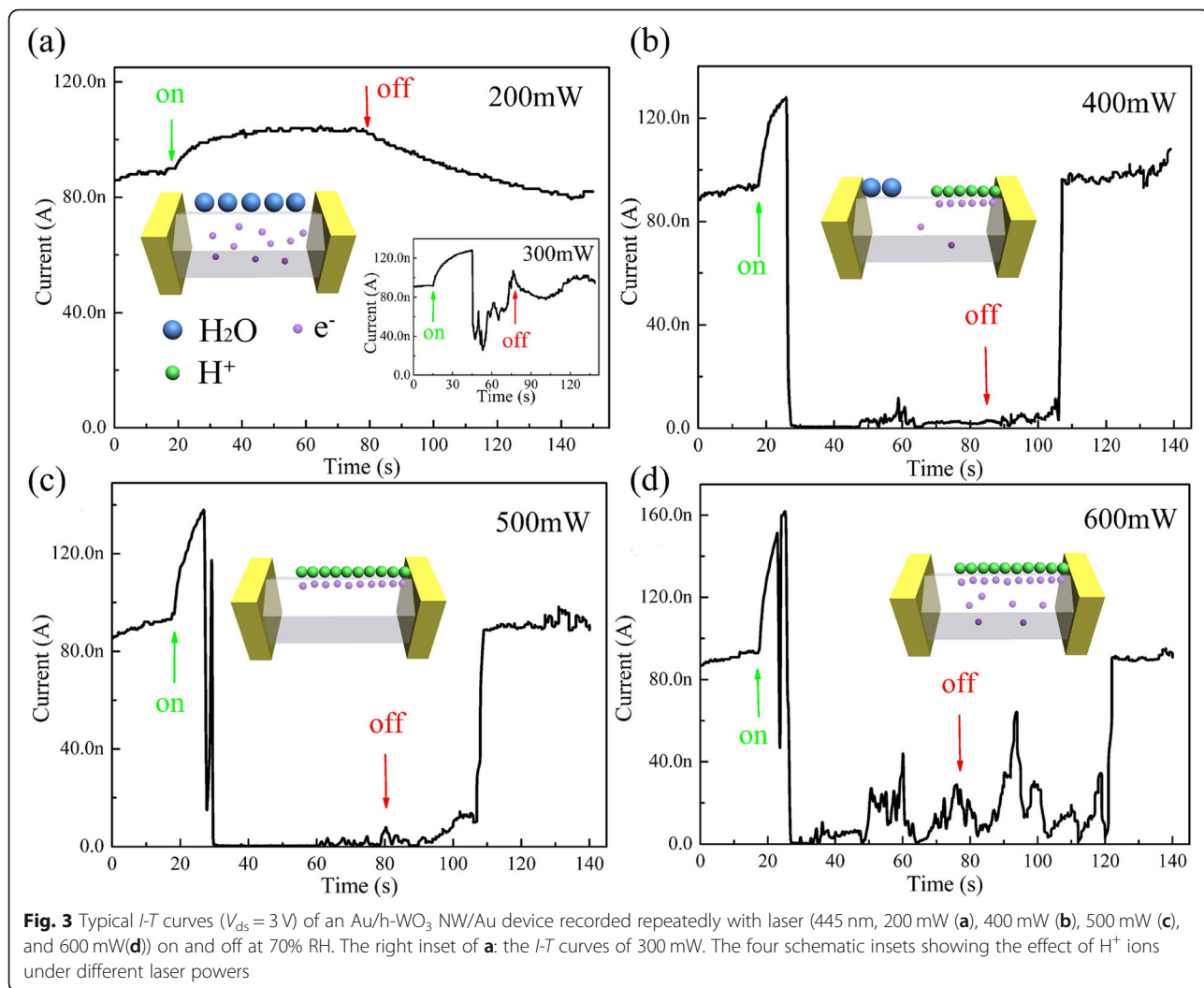
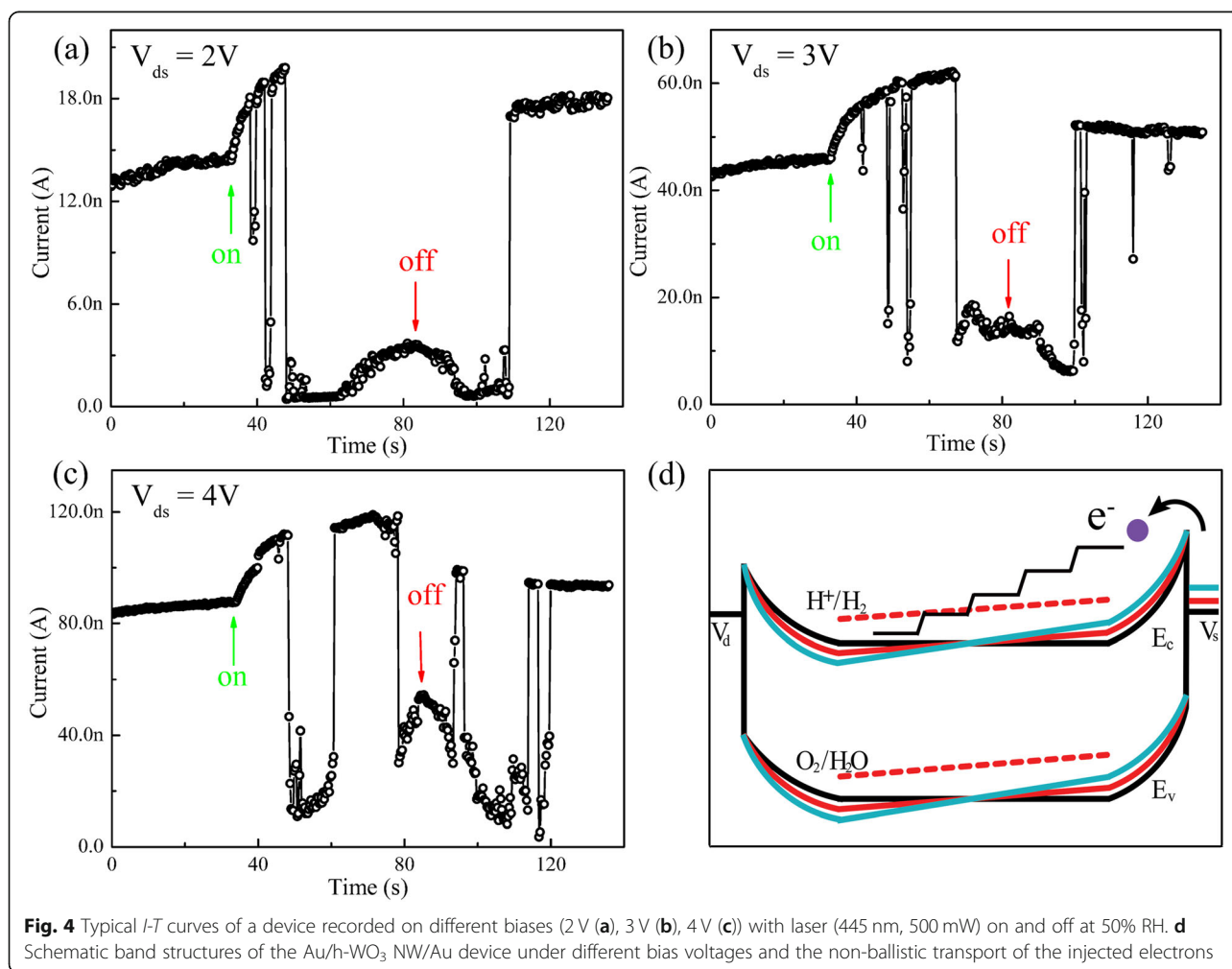


**Fig. 3** Typical  $I$ - $T$  curves ( $V_{ds} = 3$  V) of an Au/h-WO<sub>3</sub> NW/Au device recorded repeatedly with laser (445 nm, 200 mW (a), 400 mW (b), 500 mW (c), and 600 mW(d)) on and off at 70% RH. The right inset of a: the  $I$ - $T$  curves of 300 mW. The four schematic insets showing the effect of H<sup>+</sup> ions under different laser powers

localizing mobile electrons is weak or even negligible, and then the device exhibits the PPC effect (Fig. 1a).

To further investigate the origin of the NPC effect and confirm the reasonableness of the above mechanism, the power-dependent  $I$ - $T$  measurements were carried out systematically as shown in the Fig. 3. When the power of the laser is set at 200 mW, the device exhibits stable PPC effect under illumination (Fig. 3a). As the power increases to 300 mW, some traces of NPC can be clearly observed (the right inset of Fig. 3a). With further increasing laser power from 300 to 400 mW and 500 mW, the current rises quickly at first seconds under illumination exhibiting the PPC effect, and then drops suddenly exhibiting the NPC effect (Fig. 3b, c). Upon switching off the light source, the current does not change significantly until it increases to initial value rapidly after more than 20s. It is clear that the current increases more significantly and drops more quickly with the light intensity increasing, which might be attributed to the rate of hydrogen ion production and aggregation proportional to the light intensity. When the light intensity is weak (less than 200 mW),

the efficiency of inter-band transition is very low, and then the generated  $H^+$  ions are negligible or reduced by hot electrons. When the light intensity is strong, the concentration of carriers (electrons and holes) increases abruptly upon illumination, and then there is the generation and aggregation of hydrogen ions. The conversion from PPC to NPC can be well explained by the process of  $H^+$  ion accumulation on the surface. When the laser power further increases to 600 mW (Fig. 3d), the photocurrent fluctuates drastically, which might be attributed to the competition between the production and reduction of  $H^+$  ions. The efficiency of the inter-band transition is so high that the adsorbed  $H_2O$  molecules are consumed fast and cannot be supplied just in time. After all, it takes a certain time for the  $H_2O$  molecules in atmosphere to relax onto the h- $WO_3$  NW surface. From the above analysis, we concluded that the productivity of  $H^+$  ions is dependent on the efficiency of inter-band transition. When the power of laser is low, the efficiency of inter-band transition is relatively low, and it will take more time to produce enough  $H^+$  ions to achieve the conversion from PPC to NPC





effect. In contrast, when the power becomes larger, it will take shorter time to achieve this kind of conversion.

To further study the regulation of  $H^+$  ions and then the conversion between the PPC and NPC effect of the h- $WO_3$  NWs, the typical  $I$ - $T$  curves of an Au/h- $WO_3$  NW/Au device were measured under different bias voltages as shown in Fig. 4. In this part, the RH level is set at 50%, because the amount of the adsorbed  $H_2O$  molecules is not so much that the effect of the bias voltages might be more obvious. When the bias voltage is 2 V, the NPC in the  $WO_3$  nanowire is very stable under illumination (445 nm, 500 mW) as shown in Fig. 4a. However, with the bias voltage increasing, the  $I$ - $T$  curves become more fluctuated as displayed in the Fig. 3b, c). Meanwhile, it also indicates that it takes less time to achieve the conversion from PPC to NPC effect under the small bias voltage. In addition, when the light was switched off, the current decreases a little at first because the photo-excited electrons and holes preferentially recombine as shown in Fig. 4, which is similar to the cases in InN thin film [32] and InAs nanowire [33]. To comprehend this phenomenon completely, the electronic band structure of the Au/h- $WO_3$  NW/Au device is shown in the Fig. 4d, which bends gradually with bias voltage increasing. Though the  $H^+$  ion reduction level lies slightly higher than the bottom of the conduction band of the  $WO_3$  NW, the number of the hot electrons above the  $H^+$  ions reduction level injected from the negatively charged electrode based on Schottky emission might be large enough as long as the bias is large enough. These hot electrons exist only near the negatively charged electrode due to their non-ballistic transport behavior and will reduce the accumulated  $H^+$  ions quickly. As the  $H^+$  ions disappear, the height of the Schottky barrier decreases, and the voltage dropping on the barrier decreases accordingly. The number of the hot electrons above the  $H^+$  ion reduction level decreases correspondingly, which will lead to the accumulation of  $H^+$  ions again. Therefore, for the relatively long h- $WO_3$  NW, it is reasonable to consider that the  $H^+$  ions accumulate and are reduced by hot electrons alternatively, which results in current fluctuating as shown in Fig. 4c.

## Conclusions

In summary, we have systematically investigated the photoelectric properties of the Au/h- $WO_3$  NW/Au devices. The experimental results indicate that the h- $WO_3$  NW presents excellent and stable NPC effect under high RH, moderate laser power, and small bias voltage. This is because the  $H^+$  ions produced by  $H_2O$  oxidation on the surface of h- $WO_3$  NW will capture mobile electrons and then reduce the concentration of carriers and will result in a significant increase in the height of interface barrier of the Au/h- $WO_3$  NW/Au device. By adjusting

the relative humidity, light intensity, or bias voltage, the concentration and distribution of  $H^+$  ions and then the conversion between positive and negative photoconductivity can be well regulated in this kind of devices. This work might help to better understand the behavior of  $H^+$  ions and offer a new possibility to regulate the optical and resistive switching properties of  $WO_3$ .

## Abbreviations

Au: Aurum;  $H^+$  ions: Hydrogen ions; h- $WO_3$ : Hexagonal tungsten trioxide;  $I$ - $T$ : Current-time;  $I$ - $V$ : Current-voltage; NPC: Negative photoconductivity; NW: Nanowire; PPC: Positive photoconductivity; RH: Relative humidity

## Funding

This work was supported by the National Science Foundation of China (NSFC) (11574081), the Natural Science Foundation of Hunan Province (2018JJ3323), and National Students' Platform for Innovation and Entrepreneurship Training Program (201810542022).

## Availability of Data and Materials

The datasets used or analyzed during the current study are available from the corresponding author on reasonable request.

## Authors' Contributions

YHL and PF performed the experiments and drafted the manuscript with the help of YL, YHP, WJ, GZ, WK, and WC. DS participated in the design of the study and helped to draft and revised the manuscript. All authors read and approved the final manuscript.

## Competing Interests

The authors declare that they have no competing interests.

## Publisher's Note

Springer Nature remains neutral with regard to jurisdictional claims in published maps and institutional affiliations.

Received: 12 February 2019 Accepted: 8 April 2019

Published online: 24 April 2019

## References

1. He YP, Wu ZY, Fu ML, Li CR, Miao YM, Cao L et al (2003) Photochromism and size effect of  $WO_3$  and  $WO_3$ - $TiO_2$  aqueous sol. *Chem Mater* 15:4039–4045
2. Yamazaki S, Ishida H, Shimizu D, Adachi K (2015) Photochromic properties of tungsten oxide/methylcellulose composite film containing dispersing agents. *ACS Appl Mater Inter* 7:26326–26332
3. He T, Yao JN (2007) Photochromic materials based on tungsten oxide. *J Mater Chem* 17:4547–4557
4. Baek SH, Choi KS, Jaramillo TF, Stucky GD, McFarland EW (2003) Enhancement of photocatalytic and electrochromic properties of electrochemically fabricated mesoporous  $WO_3$  thin films. *Adv Mater* 15:1269–1273
5. Kida T, Nishiyama A, Hua ZQ, Suematsu K, Yuasa M, Shimanoe K (2014)  $WO_3$  nanolamella gas sensor: porosity control using  $SnO_2$  nanoparticles for enhanced  $NO_2$  sensing. *Langmuir* 30:2571–2579
6. Garcia-Sanchez RF, Ahmido T, Casimir D, Baliga S, Misra P (2013) Thermal effects associated with the Raman spectroscopy of  $WO_3$  gas-sensor materials. *J Phys Chem A* 117:13825–13831
7. Wang J, Khoo E, Lee PS, Ma J (2008) Synthesis, assembly, and electrochromic properties of uniform crystalline  $WO_3$  nanorods. *J Phys Chem C* 112:14306–14312
8. Wang J, Khoo E, Lee PS, Ma J (2009) Controlled synthesis of  $WO_3$  nanorods and their electrochromic properties in  $H_2SO_4$  electrolyte. *J Phys Chem C* 113:9655–9658
9. Santato C, Odziemkowski M, Ulmann M, Auustynski J (2001) Crystallographically oriented mesoporous  $WO_3$  films: synthesis, characterization, and applications. *J Am Chem Soc* 123:10639–10649
10. Lee SH, Deshpande R, Parilla PA, Jones KM, To B, Mahan AH et al (2006) Crystalline  $WO_3$  nanoparticles for highly improved electrochromic applications. *Adv Mater* 18:763–766

11. Lei L, Yin YL, Liu C, Zhou Y, Peng YH, Zhou F et al (2017) Resistive switching behavior of hexagonal sodium tungsten bronze nanowire. *Solid State Ionics* 308:107–111
12. Le VQ, Do TH, Retamal JRD, Shao PW, Lai YH, Wu WW, He JH, Chueh YL, Chu YH (2019) Van der Waals heteroepitaxial AZO/NiO/AZO/muscovite (ANA/muscovite) transparent flexible memristor. *Nano Energy* 56:322–329
13. Retamal JRD, Ho CH, Tsai KT, Ke JJ, He JH (2019) Self-organized Al Nanotip electrodes for achieving ultralow-power and error-free memory. *IEEE Trans Electron Devices* 66:948–943
14. Cong S, Geng FX, Zhao ZG (2016) Tungsten oxide materials for optoelectronic applications. *Adv Mater* 28:10518–10528
15. Zhou Y, Peng YH, Yin YL, Zhou F, Liu C, Ling J et al (2016) Modulating memristive performance of hexagonal WO<sub>3</sub> nanowire by water-oxidized hydrogen ion implantation. *Sci Rep* 6:32712
16. He XW, Yin YL, Guo J, Yuan HJ, Peng YH, Zhou Y et al (2013) Memristive properties of hexagonal WO<sub>3</sub> nanowires induced by oxygen vacancy migration. *Nanoscale Res Lett* 8:50
17. Liu BQ, Tang DS, Zhou Y, Yin YL, Peng YH, Zhou WC et al (2014) Electrical characterization of H<sub>2</sub>S adsorption on hexagonal WO<sub>3</sub> nanowire at room temperature. *J Appl Phys* 116:164310
18. Zhou Y, Yin YL, Peng YH, Zhou WC, Yuan HJ, Qin ZA et al (2014) Enhanced memristive performance of individual hexagonal tungsten trioxide nanowires by water adsorption based on Grotthuss mechanism. *Mater Res Express* 1:025025
19. Guo J, Zhou Y, Yuan HJ, Zhao D, Yin YL, Hai K et al (2013) Reconfigurable resistive switching devices based on individual tungsten trioxide nanowires. *AIP Adv* 3:042137
20. Gu ZJ, Zhai TY, Gao BF, Sheng XH, Wang YB, Fu HB et al (2006) Controllable assembly of WO<sub>3</sub> nanorods/nanowires into hierarchical nanostructures. *J Phys Chem B* 110:23829–23836
21. Serge Z, Eugene K, Benjamin C, Sivacarendran B (2014) Proton intercalated two-dimensional WO<sub>3</sub> nano-flakes with enhanced charge-carrier mobility at room temperature. *Nanoscale* 6:15029–15036
22. Huang K, Zhang Q, Yang F, He DY (2010) Ultraviolet photoconductance of a single hexagonal WO<sub>3</sub> nanowire. *Nano Res* 3:281–287
23. Ouyang WX, Teng F, He JH, Fang XS (2019) Enhancing the photoelectric performance of photodetectors based on metal oxide semiconductors by charge-carrier engineering. *Adv Funct Mater* 9:1807672
24. Huang YQ, Zhu RJ, Kang N, Du J, Xu HQ (2013) Photoelectrical response of hybrid grapheme-PbS quantum dot devices. *Appl Phys Lett* 103:143119
25. Tavares MAB, Silva MJ, Peres ML, Castro S, Soares DAW, Okazaki AK et al (2017) Investigation of negative photoconductivity in p-type Pb<sub>1-x</sub>Sn<sub>x</sub>Te film. *Appl Phys Lett* 110:042102
26. Lui CH, Frenzel AJ, Pilon DV, Lee YH, Ling X, Akselrod GM et al (2014) Trion-induced negative photoconductivity in monolayer MoS<sub>2</sub>. *Phys Rev Lett* 113:166801
27. Peng L, Zhai JL, Wang DJ, Wang P, Zhang Y, Pang S et al (2008) Anomalous photoconductivity of cobalt-doped zinc oxide nanobelts in air. *Chem Phys Lett* 456:231–235
28. Zhang Q, Jie J, Diao S, Shao Z, Zhang Q, Wang L et al (2015) Solution-processed grapheme quantum dots deep-UV photodetectors. *ACS Nano* 9:1561–1570
29. Nakanishi H, Bishop KJM, Kowalczyk B, Nitzan A, Weiss EA, Tretiakov KV et al (2009) Photoconductance and inverse photoconductance in films of functionalized metal nanoparticles. *Nature* 460:371–375
30. Agmon N (1995) The Grotthuss mechanism. *Chem Phys Lett* 244:456–462
31. Chiu FC (2014) A review on conduction mechanisms in dielectric films. *Adv Mater Sci Eng* 2014:578168
32. Wei PC, Chattopadhyay S, Yang MD, Tong SC, Shen JL, Lu CY et al (2010) Room-temperature negative photoconductivity in degenerate InN thin films with a super gap excitation. *Phys Rev B* 81:045306
33. Han YX, Zheng X, Fu MQ, Pan D, Li X, Guo Y et al (2016) Negative photoconductivity of InAs nanowire. *Phys Chem Chem Phys* 18:818–826

**Submit your manuscript to a SpringerOpen<sup>®</sup> journal and benefit from:**

- Convenient online submission
- Rigorous peer review
- Open access: articles freely available online
- High visibility within the field
- Retaining the copyright to your article

---

Submit your next manuscript at ► [springeropen.com](https://www.springeropen.com)

---